

**Chemical chaperone ameliorates pathological protein aggregation
in plectin-deficient muscle**

Lilli Winter, Ilona Staszewska, Eva Mihailovska, Irmgard Fischer,
Wolfgang H. Goldmann, Rolf Schröder, and Gerhard Wiche

SUPPLEMENTAL INFORMATION

Table of contents:

Supplemental Information

Supplemental Methods

Supplemental References

Supplemental Figures S1-7

Supplemental Movies 1 and 2

Supplemental Information

Elongated mitochondrial networks in $Plec^{-/-}$ myoblasts

Apart from desmin protein aggregation and Z-disk misalignment, plectinopathy patients as well as MCK-Cre/cKO mice show alterations in mitochondrial properties (reviewed in ref. (1)). As in cultured cell systems, such as fibroblasts, plectin deficiency manifests in alterations of mitochondrial morphology (2), we monitored mitochondrial networks in $Plec^{+/+}$ and $Plec^{-/-}$ myoblasts using cytochrome C labeling. When networks were classified as fragmented, intermediate, or tubular (see also ref. 2), the fragmented phenotype in $Plec^{-/-}$ myoblasts was found to be reduced to 12% (compared to 32% in $Plec^{+/+}$ cells) and the elongated phenotype increased to 39% (compared to 15% in $Plec^{+/+}$ cells; Supplemental Figure 3), indicating a dramatic shift from the fragmented to the elongated mitochondrial network type in mutant cells. Though any functional consequences of these morphological alterations remain to be shown, they indicate that all three major MFM hallmarks, i.e. desmin-positive protein aggregates, myofibrillar degeneration, and mitochondrial abnormalities, manifest already in immortalized $Plec^{-/-}$ myoblasts.

Alterations in IF networks in other cell types than myoblasts

The molecular mechanism(s) of protein (desmin) aggregate formation in plectin-deficient myofibers and in particular the question, whether there is a direct connection between this phenomenon and the observed increases in molecular mobility as well as solubility of desmin, remain to be solved. In this context, it is of interest to note that alterations in IF network cytoarchitecture and in dynamic and biochemical properties of IF subunit proteins have also been reported for plectin-deficient cell systems other than myoblasts. For instance, accelerated assembly, aberrant lateral filament bundling, and less compactness of vimentin IF networks (concurrent with reduced cellular stiffness and increased turnover rates of focal adhesions), are characteristics of plectin-deficient fibroblasts (3-5). Similarly, in $Plec^{-/-}$ keratinocytes, keratin IFs appeared more bundled and less flexible compared to $Plec^{+/+}$ cells, leading to IF networks of less delicate appearance and greater mesh size (6). Moreover, the lack of plectin in fibroblasts and keratinocytes concurred with a shift of their corresponding IF proteins from the insoluble (cytoskeleton-associated) to the soluble cell fraction, similar to myotubes. Effects of plectin deficiency on IF network architecture and/or functionality were observed also in endothelial, astrocyte, and Schwann cells (7, 8). These observations not only confirm plectin's crucial role as IF network organizer in general, but also support our concept that IFs that are not anchored via plectin at subcellular docking

sites become destabilized, more mobile, and presumably more accessible to posttranslational modifications, which in turn might make them more prone to aggregation.

Supplemental Methods

Cell culture

De-skinned front and hind limbs of a neonatal mouse (2-3 days) were enzymatically dissociated in 3 ml enzyme solution (0.2% collagenase I in serum-free DMEM medium containing 100 nM non-essential amino acids (NEAA), 2 mM L-glutamine, 50 U/ml penicillin and 50 µg/ml streptomycin (P/S), all reagents from Gibco) for 1.5-2 hours at 37°C with gentle agitation. The digested tissue was poured into 5 ml prewarmed medium (serum-free DMEM supplemented with NEAA, P/S, and L-glutamine), and single muscle fibers were released by gentle trituration with a glass pipette. The slurry was collected by centrifugation and washed twice in PBS (15 g for 3 minutes). After resuspension in 10 ml DMEM, large fiber bundles were allowed to settle down by gravity for 1 minute and the supernatant containing single fibers was transferred into a fresh tube and centrifuged for 5 minutes at 50 g. Finally, the pellet was re-suspended in DMEM containing 20% fetal calf serum (FCS), 10% horse serum, 1% chicken embryo extract, and P/S, and plated on Matrigel TM (BD Biosciences; diluted 1:10 in DMEM)-coated dishes for 24 hours. Myoblasts were split, pre-plated on uncoated culture dishes for up to 2 hours (to remove contaminating fibroblasts, performed at every splitting procedure), and finally cultivated in Ham's F10 medium supplemented with 20% FCS, 2.5 ng/ml basic fibroblast growth factor (bFGF, Promega), and P/S on collagen-coated (0.01% collagen in PBS) culture dishes. To induce differentiation, cultures were switched to DMEM containing 5% horse serum and P/S (differentiation medium). For treatment studies, differentiation medium was supplemented with 4-PBA (Calbiochem #567616) or TMAO (Sigma, 317594). Immortalized myoblast cell lines with passage numbers of up to 40 were used for experiments.

Mouse model and treatment

12-week-old wild-type mice homozygous for the floxed plectin allele ($Plec^{F/F}$, (9)) or conditional (MCK-Cre) striated muscle-restricted plectin knockout mice (cKO, (10)), both in a C57BL/6 background, were treated once daily with 4-PBA (200 mg/kg, i.p.) or vehicle for 10 days. The 4-PBA solution was prepared by titrating equimolar amounts of 4-phenylbutyric acid (Sigma, P21005) and sodium hydroxide to pH 7.4 (11). For measuring muscle strength, 12-week-old wild-type and MCK-Cre/CKO mice were injected with 4-PBA for 20 days, and subjected to analyses on days 10 and 20 of the treatment. Grip strength was tested using a grip strength meter (Bioseb). Mice were positioned to grab a metal mesh with either only their forelimbs or with all four limbs at once and were then pulled back applying uniform force until they released the mesh. The maximal grip strength value

(average of three measurements) was normalized to mouse weight. For the inverted mesh grid test, animals were placed on a wire mesh which was inverted, and the hangtime was measured (a maximum score of 60 sec was given if the animal did not drop off).

Antibodies

For immunofluorescence microscopy, immunoprecipitation, and immunoblotting, the following primary antibodies were used: rabbit antiserum (AS) to plectin #46 (12), guinea pig AS to plectin (Progen Biotechnic, GP21), mouse monoclonal antibodies (mAbs) to desmin (Dako, clone D33), rabbit AS to desmin (Cell Signaling, #5332), mouse mAbs to α -actinin (Sigma, EA-53), mouse mAbs to GFP (Roche, clones 7.1 and 13.1), rabbit AS to GAPDH (Sigma, G9545), mouse mAbs to cytochrome C (BD Pharmingen, clone 6H2.B4), rabbit AS to HSP27 (Abcam, ab12351), rabbit AS to α B-crystallin (Enzo Life Sciences, ADI-SPA-223F), rabbit AS to HSP70 (R&D systems, AF1663), rabbit AS to HSP90 (Cell Signaling, #4877), and mouse mAbs to mtHSP60 (BD Transduction Laboratories, #611562). For immunofluorescence microscopy primary antibodies were used in combination with goat anti-rabbit IgG Alexa fluor 647, goat anti-mouse IgG Alexa fluor 647, goat anti-rabbit IgG Alexa Fluor 488, goat anti-mouse IgG Alexa Fluor 488, donkey anti-mouse IgG Rhodamine red, donkey anti-rabbit IgG Rhodamine red, and donkey anti-guinea pig IgG Rhodamine red (all from Jackson ImmunoResearch Laboratories). For immunoblot analyses HRP-conjugated secondary antibodies were used (Jackson ImmunoResearch Laboratories).

Immunofluorescence microscopy and histology

Cells were fixed in 4% PFA, permeabilized with 0.1% Triton X-100, and immunostained as described in (2). Expression plasmids encoding full-length plectin isoforms have been described previously (13), and cells were transfected using the Amaxa nucleofactor kit for human dermal fibroblasts (VAPD-1001, Lonza). Mitochondrial networks were classified as described in (2). Teased fibers were prepared and processed as described previously (14). Thin sections (10 μ m) were obtained from soleus muscle tissue that was frozen in isopentane cooled with liquid nitrogen. The staining procedure was performed using the MOM Basic Kit (Vector Laboratories). Microscopy was performed using a LSM710 fluorescence laser scanning microscope (Zeiss) equipped with a Plan-Apochromat 63x 1.4NA objective lens. Images were recorded using the LSM710 module and the Zeiss ZEN software, and processed using the Photoshop CS4 (Adobe) software package. Areas and

mean intensity of individual fibers were analyzed using ImageJ software. H&E and SDH stainings of tissue sections were performed as described in (10).

Preparation of cell and tissue lysates

Dissected muscles were snap frozen in isopentane cooled with liquid nitrogen, ground in a mortar and homogenized in lysis buffer containing 5 mM Tris-HCl pH 6.8, 10% SDS, 0.2 M DTT, 1 mM EDTA, 100 mM NaF, 50 mM β -glycerophosphate, 2 mM Na_3VO_4 , 1 mM PMSF, and Complete mini protease inhibitor cocktail (Roche). Per 10 mg of muscle, 100 μl of the buffer was used. Homogenization was performed using a Dounce tissue grinder. The homogenate was centrifuged for 10 min at 10.000 g, the supernatant was mixed with 6x SDS sample buffer (500 mM Tris-HCl pH 6.8, 600mM DDT, 10% SDS, 0.1% Bromphenol-blue, 30% Glycerol), incubated at 95°C for 5 min, and stored at -20°C (protocol modified from ref. (15)). Cells were directly scraped off in 6x SDS sample buffer, DNA sheared by pressing the samples through a 27 gauge needle, and samples were incubated for 5 min at 95°C and stored at -20°C.

FRAP analysis

For FRAP analyses myoblasts were transfected with cDNAs expressing C-terminally tagged desmin-GFP (provided by M.C. Walter, Munich, Germany) or pEGFP-N3 CAG α -actinin 2 (α -actinin-GFP, provided by D. Fürst, Bonn, Germany) using FuGENE 6 transfection reagent (Roche), grown on laminin-coated μ -dishes (Ibidi), and differentiated for 5 or 10 days in differentiation medium with or without 1 mM sodium 4-phenylbutyrate. FRAP analyses were performed with a Zeiss LSM 710 confocal microscope, equipped with a heated stage (37°C) and constant 5% CO_2 flow, using a Plan-Apochromat 63x 1.4NA objective lens and an excitation wavelength of 488 nm. Regions of interests were bleached using the Zeiss ZEN software and fluorescent recovery was assayed up to 28 min by measuring the average intensity of the bleached areas, and normalizing the values to an unbleached reference area. The background intensity was subtracted from the bleached intensity values, the pre-bleach intensity was set equal to 1, and the intensity of the initial bleach level was set to 0. The recovery of fluorescence was plotted as a function of time after bleaching.

Co-immunoprecipitation

Differentiated myoblasts were lysed in RIPA-buffer (50 mM Tris-HCl pH 7.4, 150 mM NaCl, 1% NP-40, 0.5% sodium deoxycholate, 0.1% SDS) supplemented with Complete mini protease inhibitor cocktail (Roche). Immunoprecipitation was performed using protein G-agarose beads (Pierce).

Cell stretcher

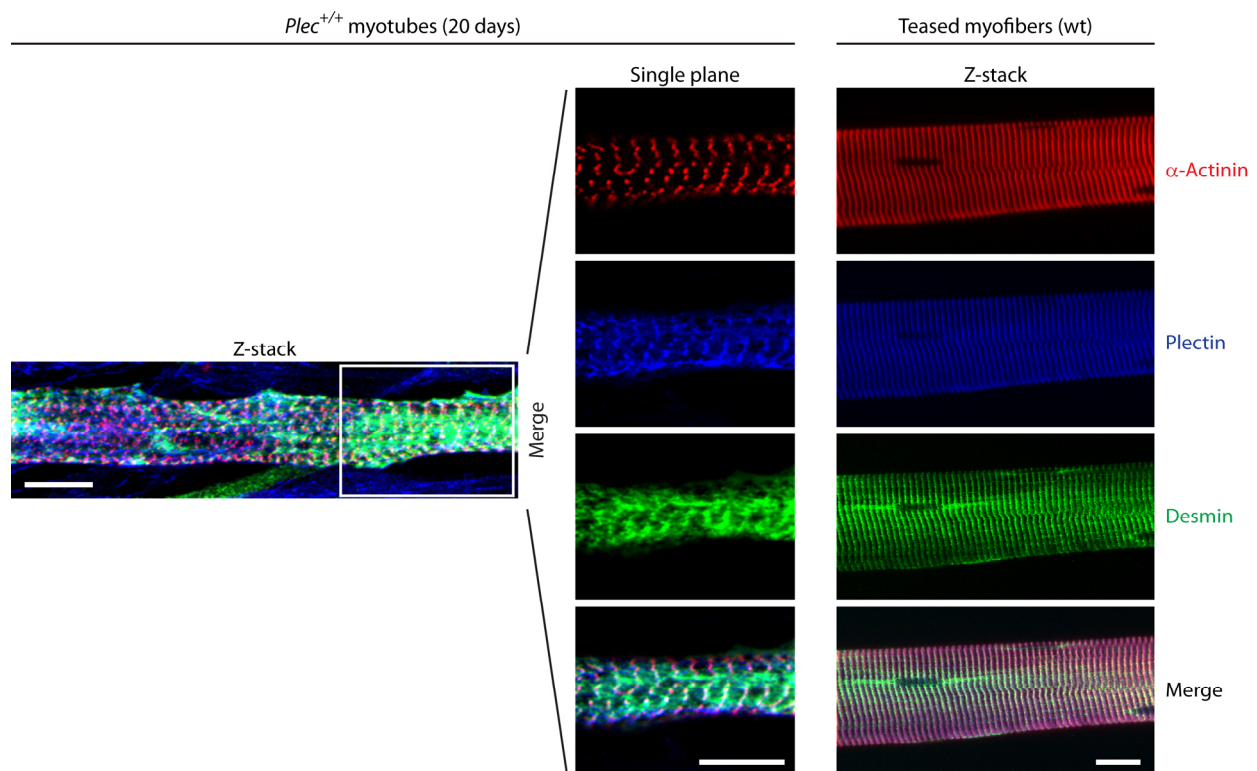
Stretch experiments were carried out on flexible polydimethylsiloxan (PDMS, Sylgard) substrates (coated with laminin) that were molded into the shape of a cell culture well with 4.0 cm² internal surface. Plated cells were differentiated for 10 days by applying differentiation medium with or without 4-PBA. PDMS gels were then attached to a direct current linear motor with an integrated gearbox (RB35, Conrad Electronic SE). Uniaxial, cyclic stretching was performed in an incubator under normal cell culture conditions for 60 min at 30% stretch amplitude (peak-to-peak) and at a frequency of 0.25 Hz with a resting period (dwell time) of 1 s between the lengthening and the shortening phase. To determine the number of cells before stretch, phase contrast images were obtained and the (x,y) position of the motorized microscope stage was recorded for later analysis of the same field-of-view position. To investigate the response of myotubes to cyclic stretch, the number of detached myotubes was analyzed by comparing images recorded before and after stretch as described in (16). The ratio of attached/detached cells was analyzed using Image J software.

Supplemental References

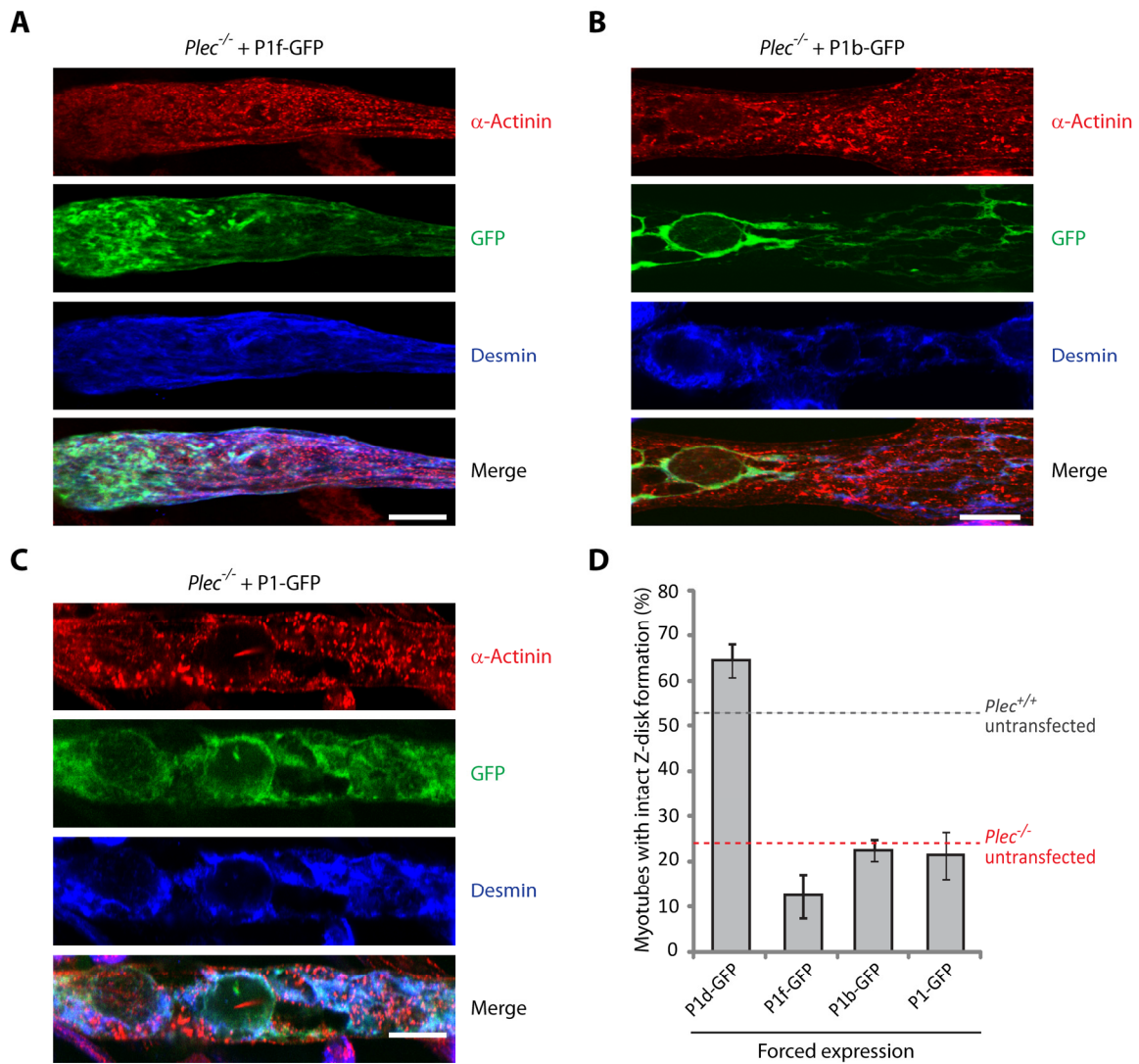
1. Winter, L., and Wiche, G. 2013. The many faces of plectin and plectinopathies: pathology and mechanisms. *Acta Neuropathol* 125:77-93.
2. Winter, L., Abrahamsberg, C., and Wiche, G. 2008. Plectin isoform 1b mediates mitochondrion-intermediate filament network linkage and controls organelle shape. *J Cell Biol* 181:903-911.
3. Spurny, R., Gregor, M., Castañón, M.J., and Wiche, G. 2008. Plectin deficiency affects precursor formation and dynamics of vimentin networks. *Exp Cell Res* 314:3570-3580.
4. Burgstaller, G., Gregor, M., Winter, L., and Wiche, G. 2010. Keeping the vimentin network under control: cell-matrix adhesion-associated plectin 1f affects cell shape and polarity of fibroblasts. *Mol Biol Cell* 21:3362-3375.
5. Na, S., Chowdhury, F., Tay, B., Ouyang, M., Gregor, M., Wang, Y., Wiche, G., and Wang, N. 2009. Plectin contributes to mechanical properties of living cells. *Am J Physiol Cell Physiol* 296:C868-877.
6. Osmanagic-Myers, S., Gregor, M., Walko, G., Burgstaller, G., Reipert, S., and Wiche, G. 2006. Plectin-controlled keratin cytoarchitecture affects MAP kinases involved in cellular stress response and migration. *J Cell Biol* 174:557-568.
7. Spurny, R., Abdourahman, K., Janda, L., Rünzler, D., Köhler, G., Castañón, M.J., and Wiche, G. 2007. Oxidation and nitrosylation of cysteines proximal to the intermediate filament (IF)-binding site of plectin: effects on structure and vimentin binding and involvement in IF collapse. *J Biol Chem* 282:8175-8187.
8. Walko, G., Wögenstein, K.L., Winter, L., Fischer, I., Feltri, M.L., and Wiche, G. 2013. Stabilization of the dystroglycan complex in Cajal bands of myelinating Schwann cells through plectin-mediated anchorage to vimentin filaments. *Glia* 61:1274-1287.
9. Ackerl, R., Walko, G., Fuchs, P., Fischer, I., Schmuth, M., and Wiche, G. 2007. Conditional targeting of plectin in prenatal and adult mouse stratified epithelia causes keratinocyte fragility and lesional epidermal barrier defects. *J Cell Sci* 120:2435-2443.
10. Konieczny, P., Fuchs, P., Reipert, S., Kunz, W.S., Zeöld, A., Fischer, I., Paulin, D., Schröder, R., and Wiche, G. 2008. Myofiber integrity depends on desmin network targeting to Z-disks and costameres via distinct plectin isoforms. *J Cell Biol* 181:667-681.

11. Ricobaraza, A., Cuadrado-Tejedor, M., Perez-Mediavilla, A., Frechilla, D., Del Rio, J., and Garcia-Osta, A. 2009. Phenylbutyrate ameliorates cognitive deficit and reduces tau pathology in an Alzheimer's disease mouse model. *Neuropsychopharmacology* 34:1721-1732.
12. Andrä, K., Kornacker, I., Jörgl, A., Zörer, M., Spazierer, D., Fuchs, P., Fischer, I., and Wiche, G. 2003. Plectin-isoform-specific rescue of hemidesmosomal defects in plectin (-/-) keratinocytes. *J Invest Dermatol* 120:189-197.
13. Rezniczek, G.A., Abrahamsberg, C., Fuchs, P., Spazierer, D., and Wiche, G. 2003. Plectin 5'-transcript diversity: short alternative sequences determine stability of gene products, initiation of translation and subcellular localization of isoforms. *Hum Mol Genet* 12:3181-3194.
14. Rezniczek, G.A., Konieczny, P., Nikolic, B., Reipert, S., Schneller, D., Abrahamsberg, C., Davies, K.E., Winder, S.J., and Wiche, G. 2007. Plectin 1f scaffolding at the sarcolemma of dystrophic (mdx) muscle fibers through multiple interactions with beta-dystroglycan. *J Cell Biol* 176:965-977.
15. Chopard, A., Pons, F., Charpiot, P., and Marini, J.F. 2000. Quantitative analysis of relative protein contents by Western blotting: comparison of three members of the dystrophin-glycoprotein complex in slow and fast rat skeletal muscle. *Electrophoresis* 21:517-522.
16. Bonakdar, N., Luczak, J., Lautscham, L., Czonstke, M., Koch, T.M., Mainka, A., Jungbauer, T., Goldmann, W.H., Schröder, R., and Fabry, B. 2012. Biomechanical characterization of a desminopathy in primary human myoblasts. *Biochem Biophys Res Commun* 419:703-707.

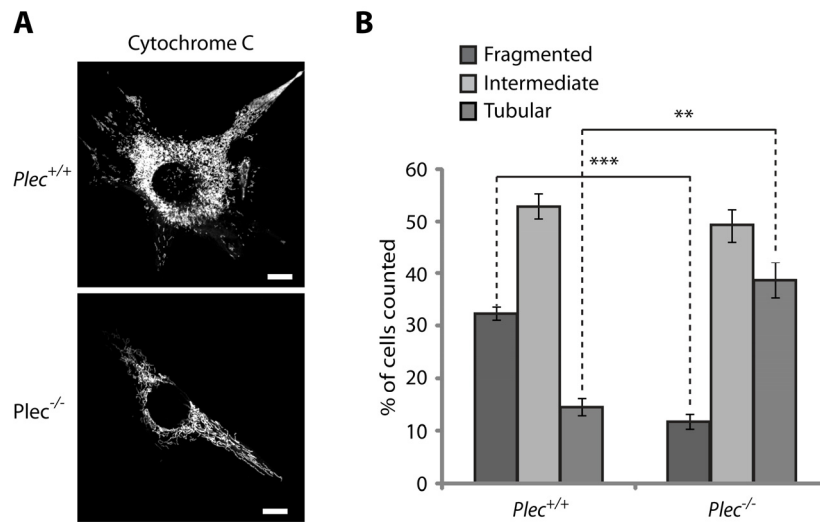
Supplemental Figures



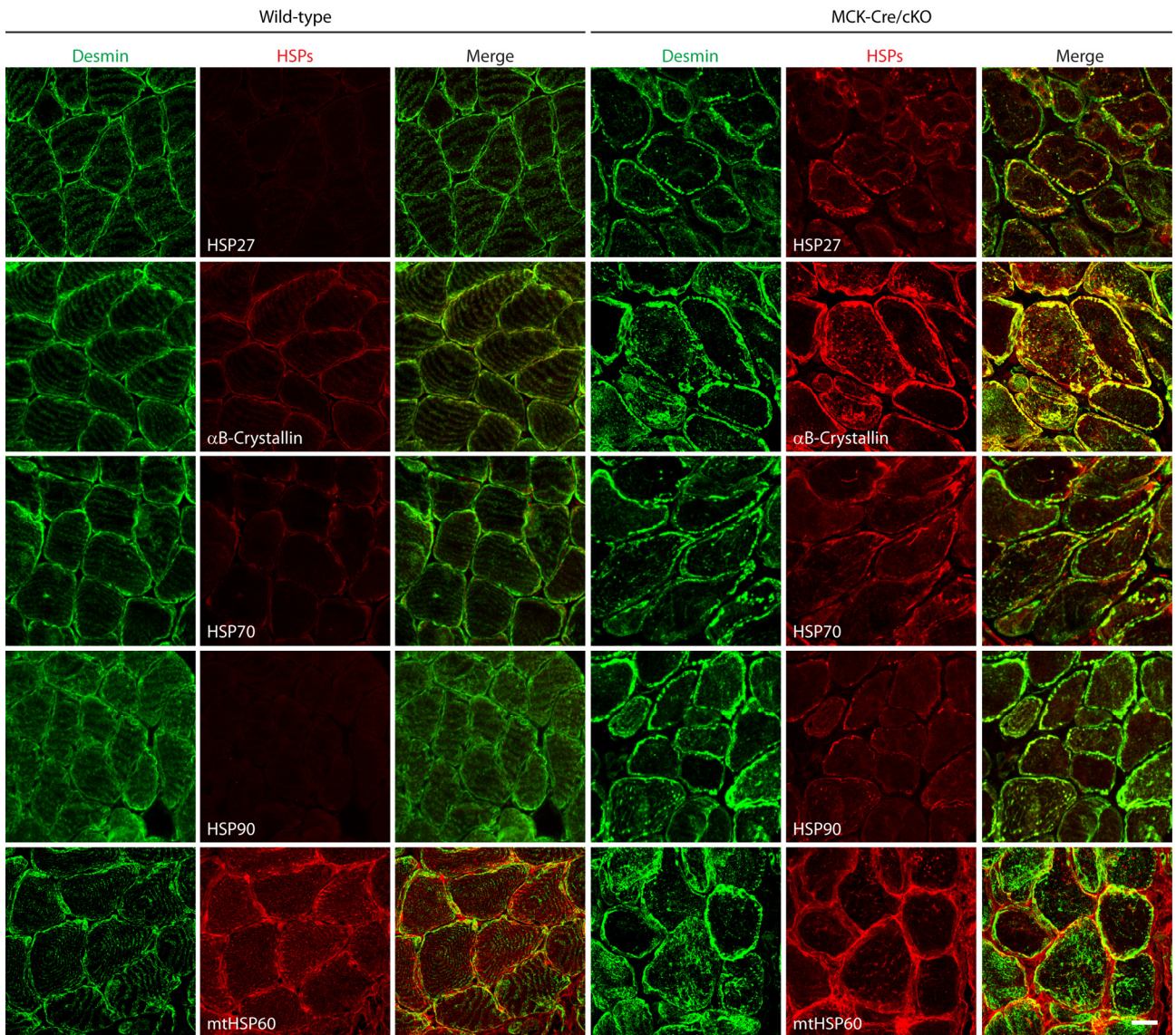
Supplemental Figure 1. Colocalization of plectin with desmin and α -actinin in *Plec*^{+/+} myotubes. Immunofluorescence microscopy of *Plec*^{+/+} myotubes differentiated for 20 days using antibodies to desmin, α -actinin, and plectin (guinea pig pan-plectin AS). A maximum intensity projection (Z-stack) is depicted. A single plane out of the Z-stack image corresponding to the boxed area is shown enlarged and in single channel mode (middle column). Single fibers teased from whole muscle immunolabeled using the same set of antibodies are shown for comparison (right column). Note that myoblast cell cultures differentiate to a state that closely resembles mature muscle fibers. Bars, 10 μ m (myotubes) and 20 μ m (teased myofibers).



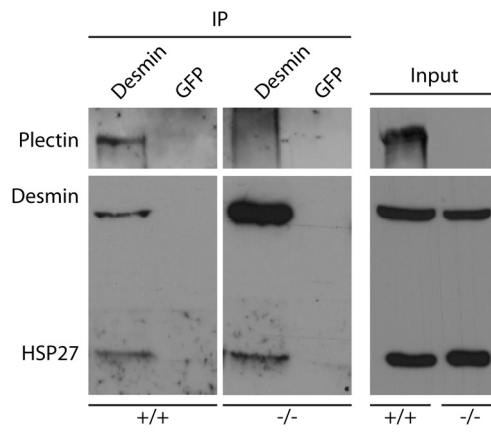
Supplemental Figure 2. Forced expression of individual plectin isoforms in *Plec*^{-/-} myotubes. **(A-C)** *Plec*^{-/-} myoblasts transfected with expression plasmids encoding fusion proteins of P1f **(A)**, P1b **(B)**, or P1 **(C)**, with C-terminal EGFP tags, were differentiated for 10 days and immunolabeled using antibodies to desmin and α -actinin. Note the colocalization of desmin with plectin isoforms, indicating recruitment of IF networks to the subcellular localization of the isoforms. Z-disk formation was not restored. Bars, 10 μ m. **(D)** Statistical analyses of *Plec*^{-/-} myotubes displaying Z-disks after individual forced expression of P1d (n=72), P1f (n=68), P1b (n=57), or P1 (n=68). Mean values \pm SEM, 3 experiments.



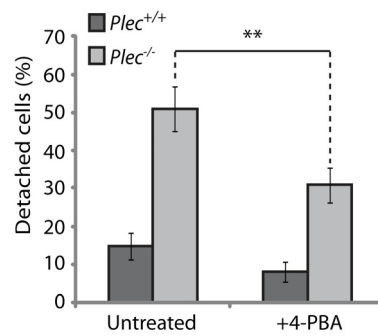
Supplemental Figure 3. Alterations of mitochondrial network morphology in *Plec*^{-/-} myoblasts. **(A)** Immunofluorescence microscopy of *Plec*^{+/+} and *Plec*^{-/-} myoblasts using antibodies to cytochrome C. Note the elongated shape of mitochondria in *Plec*^{-/-} compared to *Plec*^{+/+} cells. Bars, 10 μ m. **(B)** Statistical analysis of mitochondria classified as fragmented, tubular, or intermediate. Mean values \pm SEM, 4 experiments (*Plec*^{+/+} (n=133) and *Plec*^{-/-} (n=117) myoblasts).



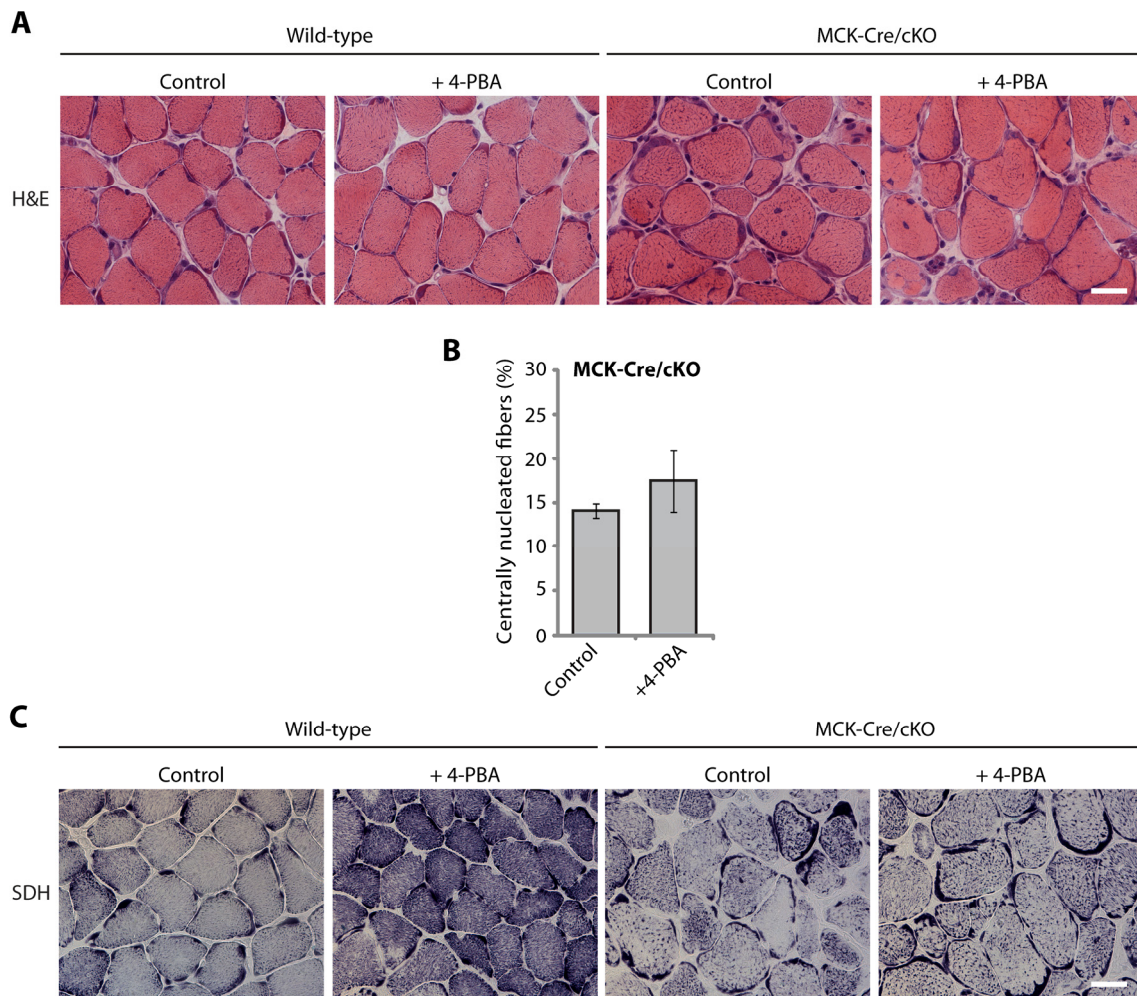
Supplemental Figure 4. Immunolocalization of chaperones in wild-type and plectin-deficient muscle fibers. (A-E) Cryosections of soleus muscles from 3-month-old wild-type and MCK-Cre/cKO mice were double-immunolabeled using antibodies to desmin and HSPs as indicated in frames. Note the massive formation of desmin aggregates in plectin-deficient muscle fibers and their partial co-localization with HSPs (except for mitochondrial HSP60). Bar, 20 μ m.



Supplemental Figure 5. Co-immunoprecipitation of desmin and HSP27. Cell lysates of differentiated *Plec*^{+/+} and *Plec*^{-/-} myoblasts (input) were subjected to immunoprecipitation using antibodies to desmin (IP), or GFP (as a control), and precipitated proteins were detected by immunoblotting using antibodies to proteins as indicated.



Supplemental Figure 6. 4-PBA treatment of differentiated *Plec*^{-/-} myotubes decreases mechanical vulnerability. *Plec*^{+/+} and *Plec*^{-/-} myoblasts, differentiated for 10 days \pm 1mM 4-PBA on PDMS gels, were subjected to cyclic stretching at 30% stretch and 0.25 Hz for 1 hour. Note that increased numbers of *Plec*^{-/-} myotubes detached after stretch compared to *Plec*^{+/+} cells (left panel). When myotubes were differentiated in medium with 1mM 4-PBA, *Plec*^{-/-} cells were less prone to stretch-induced detachment (left panel). Mean values \pm SEM, from 3 experiments each are shown (untreated: *Plec*^{+/+} n=150, *Plec*^{-/-} n=150; 4-PBA-treated: *Plec*^{+/+} n= 150, *Plec*^{-/-} n=150 myotubes). Statistical significance was determined using an unpaired Student's t-test (**, P<0.01).



Supplemental Figure 7. H&E and succinate dehydrogenase (SDH)-specific staining of skeletal muscle tissue after 10 days of 4-PBA treatment. **(A)** H&E analysis of soleus muscles derived from 12-week-old wild-type and MCK-Cre/cKO mice that had been injected with 4-PBA or vehicle (control) for 10 days. **(B)** Statistical analyses of centrally nucleated fibers in soleus muscle derived from MCK-Cre/cKO mice treated or not treated with 4-PBA (control: n=1089; treated: n=1724 fibers). Note that no differences were observed between 4-PBA-treated and untreated animals. Mean values \pm SEM, 4 experiments. **(C)** Soleus cross sections were stained for SDH. Note mitochondrial alterations in MCK-Cre/cKO muscle compared to wild-type tissue. However, no differences were observed upon treatment with 4-PBA compared to untreated MCK-Cre/cKO specimens. Bars (A, C), 20 μ m.

Supplemental Movies

Supplemental movie 1. Spontaneous contractions of *Plec*^{+/+} myotubes. *Plec*^{+/+} myoblasts were differentiated for 10 days. Note, after 7-8 days of differentiation, spontaneous contractions became apparent in the culture dish.

Supplemental movie 2. Spontaneous contractions of *Plec*^{-/-} myotubes. *Plec*^{-/-} myoblasts were differentiated for 10 days. Note that after 7-8 days of differentiation, spontaneous contractions became apparent in the culture dish.